A Technical Appendices and Supplementary Material

A.1 Interoception

The brain senses, integrates, predicts, and regulates bodily states through bidirectional communication with the internal organs. This process is known as interoception. Beyond regulating physiological responses and maintaining homeostasis, interoception also influences our motivation and emotions and affects decisions and behaviors. Its functionality relies on both neuronal pathways in the peripheral and central nervous system, as well as the circulating hormones. In the central nervous system, several experimental studies have shown that interoceptive afferent signals are first processed by subcortical nuclei, such as the nucleus of the solitary tract (NTS), the parabrachial nucleus (PBN), the locus coeruleus (LC), and the ventral posteromedial nucleus of the thalamus (VPM). These signals are further integrated by the cortical areas. In particular, the insular cortex (IC) serves as a key sensory hub for integrating bodily signals and relaying them to higher-order brain regions, including the amygdala (AMY), orbitofrontal cortex (OFC), anterior cingulate cortex (ACC), and prefrontal cortex (PFC). Finally, these signals project back to the lower brainstem and convey efferent motor commands to visceral organs, allowing for top-down regulation of the internal organs.

Here, we provide a comprehensive list of brain regions mentioned in the paper and figure. ACC: anterior cingulate cortex, AIC: anterior insular cortex, dlPFC: dorsal lateral prefrontal cortex, DVC: dorsal vagal complex, IPC: inferior parietal cortex, MCC: mid cingulate cortex, M1: primary motor cortex, NG: nodose ganglion, PAC: primary auditory cortex, PIC: posterior insular cortex, PCC: posterior cingulate cortex, S1: primary sensory cortex, TPO: temporal-parietal-occipital junction, V1: primary visual cortex, MT: mid temporal area.

A.2 Canonical Correlation Analysis for Brain-Body Association

We perform CCA to map the interoceptive network. Specifically, we first linearly reconstruct the rs-fMRI time series and then estimate the Pearson correlation coefficients between the true and reconstructed time series. Below, we provide a mathematical derivation of the reconstruction of the rs-fMRI time series.

Take the vertices at the cortical surface as an example. We estimate their covariance with the context vector $\mathbf{c}$ as **COV** and perform SVD to get singular vectors $\mathbf{U}$ and $\mathbf{V}$, and singular values Σ, following

$$\mathbf{COV} = \mathbf{U}\Sigma\mathbf{V}^T.$$

Assuming that $\mathbf{X}$ and $\mathbf{Y}$ are brain activity with the shape of (n_{voxels}, n_{times}) and bodily representations with the shape of (n_{dims}, n_{times}), respectively, we project $\mathbf{X}$ and $\mathbf{Y}$ to the shared space following

$$\mathbf{X}_{proj} = U[:, 0:n]^T\mathbf{X},$$

$$\mathbf{Y}_{proj} = \Sigma[0:n, 0:n]V[:, 0:n]^T\mathbf{Y},$$

where n is the number of singular vectors ($n = 4$) chosen empirically, and $\mathbf{X}_{proj}$ and $\mathbf{Y}_{proj}$ are projected signals. Given that two projected signals are in the same shared space, we can combine the above two equations into

$$U[:, 0:n]^T\mathbf{X} \approx \Sigma[0:n, 0:n]V[:, 0:n]^T\mathbf{Y}.$$

Its reorganization leads to

$$\mathbf{X} \approx U[:, 0:n]\Sigma[0:n, 0:n]V[:, 0:n]^T\mathbf{Y}.$$

Therefore, we can approximately reconstruct or predict the brain activity ($\hat{\mathbf{X}}$) based on its co-fluctuation with the bodily states, with the following equation

$$\hat{\mathbf{X}} = U[:, 0:n]\Sigma[0:n, 0:n]V[:, 0:n]^T\mathbf{Y}.$$

We calculate the Pearson correlation coefficients between the reconstructed brain activities and the true brain activities for all vertices on the cortical surface across all subjects in the test set. Brain regions with higher correlation coefficients fluctuate similarly with the physiological signals, thus better encoding bodily states.

A.3 Statistical Analysis

The singular vectors in $\mathbf{U}$ reveal the brain patterns that co-fluctuate with the physiological signals. We estimate and visualize the top four singular vectors from the cortical and subcortical spaces, separately. Specifically, we first calculate the covariance (1) between the context vectors $\mathbf{c}$ and every vertice in the cortical surface, or (2) between the context vectors $\mathbf{c}$ and every voxel in the subcortical space, followed by SVD to get singular vectors $\mathbf{U}$. Each element in a singular vector represents the value of a voxel, mapping its association with the bodily states. We perform a blocked permutation test to highlight voxels with associations that are higher than the chance level. To obtain the null distribution, we randomly permute the rs-fMRI test series 1,000 times, using a block size of 45 seconds, and repeat the procedure to estimate the singular vectors. The significance level (α) is 0.05. Additionally, we perform the Benjamini-Hochberg procedure to correct for multiple comparisons and control the false positive rate.

A.4 Organ-Specific Association with Brain

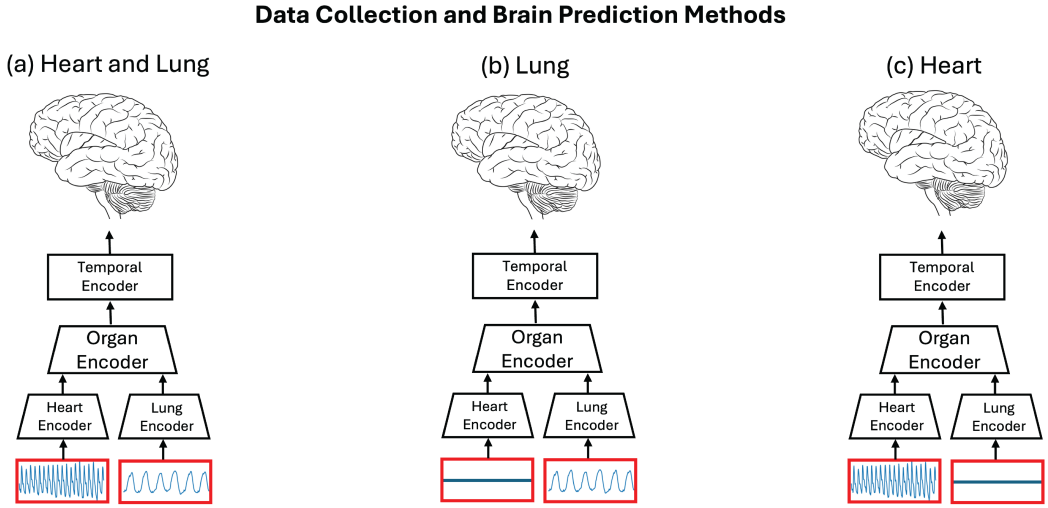

Figure 4: The framework to reconstruct or predict brain activities from context vectors. (a) Both cardiac input and respiratory input are provided to the model to extract the context vectors for reconstructing brain activities. (b) Only respiratory input is provided to the model to extract the context vectors for reconstructing brain activities. Zero values are used to replace the cardiac input. (c) Only cardiac input is provided to the model to extract the context vectors for reconstructing brain activities. Zero values are used to replace the respiratory input. Using this framework, we estimate the interoceptive network that encodes both cardiac and respiratory input from (a), only respiratory input from (b), and only cardiac input from (c).

We isolate the organ-specific contribution to the interoceptive network and explore whether organ-specific mapping exists in the brain. Fig. 4 details the method. For example, we isolate the brain regions with activities that only fluctuate with the respiratory signals by silencing the cardiac input (Fig. 4b). The model takes segments of the true respiratory trace and fake cardiac input (zero values) and outputs corresponding context vectors $\mathbf{c}$. We repeat the CCA (detailed in A.2) between these context vectors $\mathbf{c}$ and rs-fMRI signals in the cortical space. In this way, we map the brain regions with activities that fluctuate only with the respiratory signal, but not with the cardiac signals. A

similar approach can isolate the brain regions with activities that fluctuate only in response to cardiac signals. Taken together, we leverage the power of the proposed model to map the organ-specific and organ-sharing brain regions in the interoceptive network.

A.5 Supplementary Results

A.5.1 Common Space for Brain and Body Fluctuations

Brain activities fluctuate with bodily states in shared space. The top several singular vectors, estimated from the covariance matrix between the two, span the shared space. In this study, we select four singular vectors to form the axis of the shared space. In particular, the first singular vectors $\mathbf{u}_1$ and $\mathbf{v}_1$, along which the most aligned activities between the brain and the body are observed. The alignments between projected signals along the first singular vectors are shown in Fig. 5. Note that the analysis at the cortical and subcortical levels is performed separately. We independently calculate the covariance matrices for cortical signals and subcortical signals, and estimate their singular vectors to yield two separate shared spaces related to bodily states. However, the projected bodily states in two spaces align well with each other, and so do the projected cortical and subcortical activities. This observation shows that these two shared spaces highly agree with each other, potentially indicating a three-way co-fluctuation between the cortical, subcortical activities, and bodily states.

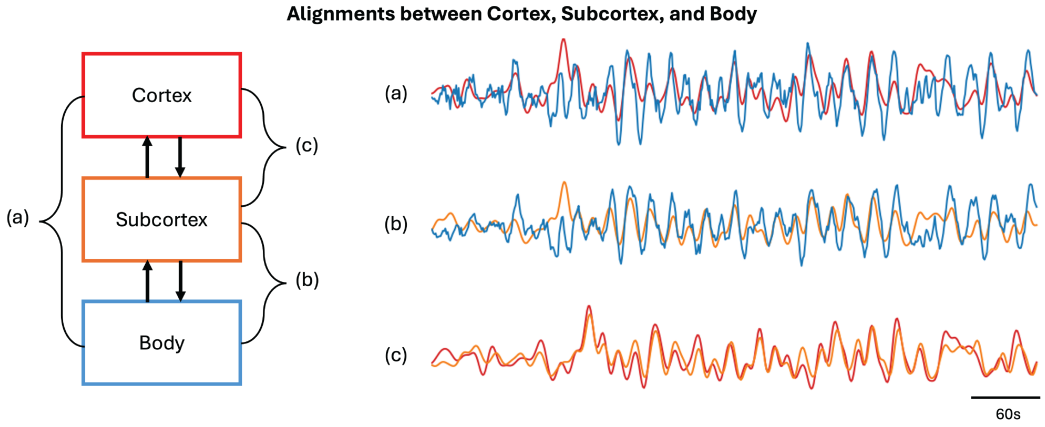

Figure 5: Projections of rs-fMRI and physiological signals to the shared space spanned by the first singular vectors. Signals from the brain and the body are better aligned in the shared space. (a) Alignment between the projected cortical activities and bodily states (context vectors), (b) Alignment between the projected subcortical activities and bodily states (context vectors), (c) Alignment between the projected cortical and subcortical activities.

A.5.2 Cortical Brain Maps

We visualize the top four singular vectors $\mathbf{u}_1$ to $\mathbf{u}_4$ in the cortical space in Fig.6. The patterns highlight the insular cortex, the somatosensory cortex, and the visual and auditory cortex. Compared with $\mathbf{u}_1$ and $\mathbf{u}_2$, $\mathbf{u}_3$ and $\mathbf{u}_4$ highlight more find-grained brain regions.

A.5.3 Subcortical Brain Maps

We visualize the first singular vectors $\mathbf{u}_1$ in the subcortical space in Fig.7. The patterns highlight the thalamus, hippocampus, and brainstem.

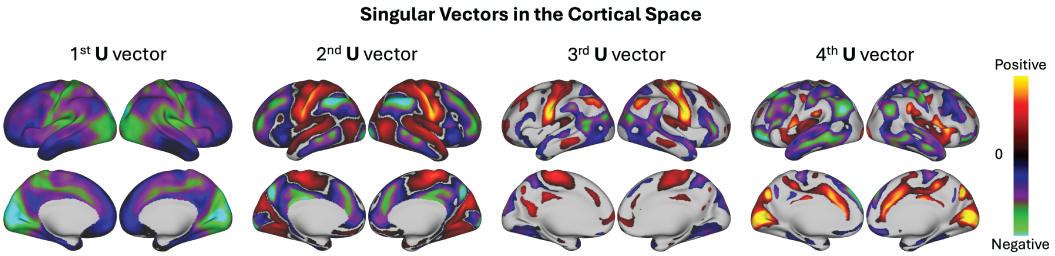

Figure 6: The top four singular vectors in $\mathbf{U}$ are visualized in the cortical space. Only vertices with a statistically significant difference from the null distribution are displayed ($p < 0.05$).

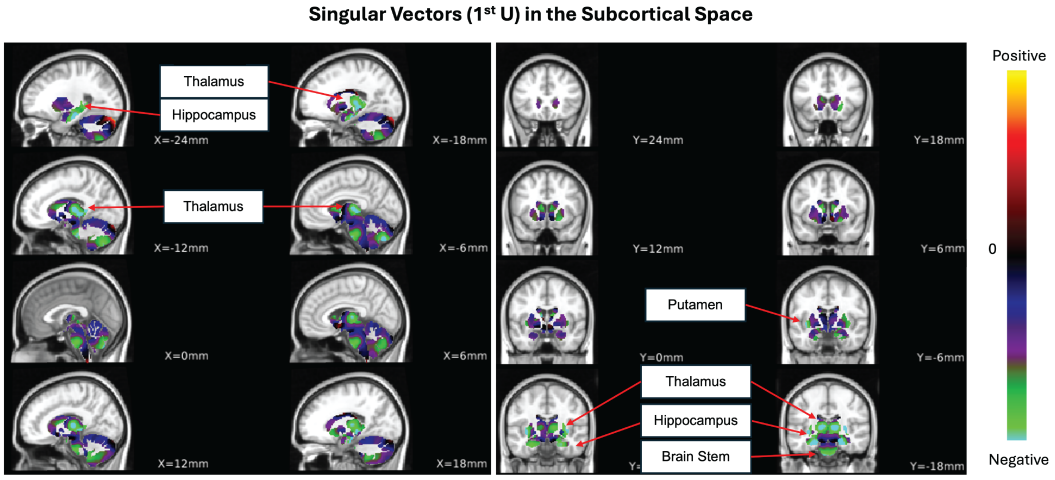

Figure 7: The first singular vector in $\mathbf{U}$ is visualized in the subcortical space. Only voxels with a statistically significant difference from the null distribution are displayed ($p < 0.05$).